TECHNICAL TRANSACTIONS | CZASOPISMO TECHNICZNE
CIVIL ENGINEERING | BUDOWNICTWO

2-B/2015

ADAM ZABORSKI*

SIMULATION OF CONCRETE CORROSION AND INTERACTION SURFACES USING CELLULAR AUTOMATA

SYMULACJA KOROZJI BETONU I POWIERZCHNI INTERAKCJI AUTOMATAMI KOMÓRKOWYMI

Abstract

This paper presents a new approach to determining the synergetic effects of environmental conditions and mechanical loading on the load bearing capacity of structural members. Cellular automata are used to estimate the residual strength of a RC section subjected to concrete corrosion. The evolution of interaction surfaces resulting from bending moments and axial force caused by a continuous degradation process is presented.

Keywords: concrete corrosion, cellular automata, continuum damage mechanics, cross-section bearing capacity

Streszczenie

W artykule przedstawiono próbę oszacowania skutków oddziaływania środowiska i mechanicznego obciążenia na nośność elementów konstrukcji. Postępy korozji betonu i rezydualną wytrzymałość przekroju żelbetowego określono automatami komórkowymi. Przedstawiono ewolucję powierzchni interakcji momentów gnących i siły osiowej spowodowaną postępującymi procesami degradacji.

Słowa kluczowe: korozja betonu, automaty komórkowe, kontynualna mechanika uszkodzeń, nośność przekroju

DOI: 10.4467/2353737XCT.15.144.4181

* Institute of Structural Mechanics, Cracow University of Technology, Poland.

1. Introduction

The deterioration of concrete under combined environmental actions and mechanical loading involves different mechanisms acting on different scales, from the nanometer to the meter level, [11]. The governing equations used to describe the processes at the molecular level are usually averaged statistically at the mesoscale. Due to the limited possibilities of laboratory testing, the process parameters are determined at the macro scale. As a result, the understanding of the process mechanisms is blurred and the parameters are averaged over a representative volume. The use of averaged values leads to a phenomenological description where the bulk behaviour of the body can be explained statistically and applied to macroscopic state variables.

This paper deals with a phenomenological model of stress-assisted concrete corrosion. It presents constitutive equations for the viscoelastic continuum and multicomponent transport through porous material. The deterioration of material is described by a scalar parameter split into chemical and mechanical parts. For each part, a proper evolution equation is adopted. Compound chemical and mechanical deterioration allows the prediction of the stress state in the material. To transpose these results onto the real scale of structural members, the stress is integrated over a cross-section. The bearing capacity of the partially damaged cross-section is simulated numerically. The ultimate limit state, prescribed by Eurocode 2, provides the interaction surfaces of the cross-sectional forces. Evolution of these surfaces over time exemplifies the change of the cross-section bearing capacity. Almost all numerical simulations are carried out by a novel method of cellular automata. In this method, the space is divided into identical cells. The simulation relies on a series of actualization of cell states on the basis of an automation rule – this is identical for all the cells and uses the state of neighboring cells. For more information about cellular automata, please see [12].

In the paper, the main characteristics of the proposed model are reported succinctly, while more attention is paid to the construction of interaction curves.

2. Constitutive equations

2.1. Concrete matrix

Concrete is considered to be a viscoelastic material with fading memory. The creep of the material in response to loading can be described by the hereditary theory in the form of Volterra integral equation of the second type [1]:

$$\varepsilon(t) = \frac{\sigma(t)}{E(t)} - \int_{\tau_o}^{t} J(t,\tau)\sigma(\tau)d\tau \tag{1}$$

where σ is the effective stress, and the compliance function J can be expanded in a Dirichlet series:

$$J(t,\tau)=\sum_{i=1}^{k} f_i(t)g_i(\tau) \tag{2}$$

which leads to a generalized Kelvin chain with a series arrangement. This is equivalent to the second order differential equation but is in contradistinction to the generalized Maxwell chain where each element sustains the same stress value. This achieves two goals. Firstly, the constitutive laws for a viscoelastic material can be written in terms of a limited number of internal variables. Secondly, a recurrent definition of internal variables can be introduced, [1, 13]:

$$Y_0^{(k)}=0\,,\quad Y_i^{(k)}=Y_{i-1}^{(k)}+\int_{t_i}^{t_{i+1}}\sigma(\tau)g_k(\tau)d\tau \tag{3}$$

and limited to two elements of the chain:

$$\begin{aligned}\varepsilon(t_{i+1})&=\varepsilon(t_i)+\frac{\sigma(t_{i+1})}{E(t_{i+1})}-\frac{\sigma(t_i)}{E(t_i)}+\\&+[e^{-\gamma t_{i+1}}-e^{-\gamma t_i}]\mathbf{Y}_{i-1}+\int_{t_i}^{t_{i+1}}\sigma(\tau)[g_1(\tau)+e^{-\gamma t_{i+1}}g_2(\tau)]d\tau\end{aligned} \tag{4}$$

and only one internal variable in each calculation point takes into account the history of the process. This reduces the number of numerical operations and demands on computer memory. Therefore, a remark in Cervera et al. [2] about the integral approach being unsuitable for numerical computation does not seem to be justified in a general sense.

The material behaviour is not dependent on ongoing diffusion processes. The effects of liquid and gas pressure are not included.

2.2. Transport equations

The mixture theory describes the behaviour of simultaneous multicomponent flows that occur inside the material. The mass balance equations for each constituent concentration c_i result in a set of Fick's second law equations:

$$\begin{aligned}\rho\frac{\partial c_i}{\partial t}&=\underbrace{-\rho\mathbf{w}\cdot\mathbf{grad}c_i}_{\text{convection}}+\underbrace{\mathrm{div}\sum_{k=1}^{m}\overline{D}_{ik}\mathbf{grad}\sigma_k}_{\text{pressure diffusion}}+\underbrace{\mathrm{div}\sum_{k=1}^{n-1}D_{ik}\mathbf{grad}c_k}_{\text{conc.diffusion}}-\\&\underbrace{-\mathrm{div}\sum_{k=1}^{n-1}L_{ik}\left(\mathbf{F}_k-\mathbf{F}_n\right)}_{\text{ext.forces}}+\underbrace{r_i}_{\text{sources}}\end{aligned} \tag{5}$$

where some terms can be neglected. The terms of pressure diffusion and external forces are irrelevant for free inflow of aggressive species, and when the Peclet number is much smaller than one, the transport processes are diffusion driven and the convection term can be omitted, [5, 9]. The actual form of diffusion equations:

$$\rho\frac{\partial c_i}{\partial t}=\mathrm{div}\sum_{k=1}^{n-1}D_{ik}\,\mathbf{grad}c_k+r_i \tag{6}$$

serves as the basis for the determination of components concentration. The above formulae describe conjugated as well as coupled flows. Using the concept of cellular automata, [14], equations (6) can be written as:

$$\begin{aligned}c_{m,n}^{\alpha(1)}&=c_{m,n}^{\alpha(0)}\left(1-a^{\alpha}\right)+\frac{a^{\alpha}}{4}\left(c_{m+1,n}^{\alpha(0)}+c_{m,n+1}^{\alpha(0)}+c_{m-1,n}^{\alpha(0)}+c_{m,n-1}^{\alpha(0)}\right)-\\&-\sum_{\beta\neq\alpha}a^{\alpha\beta}c_{m,n}^{\beta}+\sum_{\beta\neq\alpha}\frac{a^{\alpha\beta}}{4}\left(c_{m+1,n}^{\beta(0)}+c_{m,n+1}^{\beta(0)}+c_{m-1,n}^{\beta(0)}+c_{m,n-1}^{\beta(0)}\right)\end{aligned} \tag{7}$$

$$a^{\alpha\beta}=\frac{4D_{\alpha\beta}\Delta t}{h^2} \tag{8}$$

using the von Neumann automaton rule, and:

$$\begin{aligned}c_{m,n}^{\alpha(1)}&=c_{m,n}^{\alpha(0)}\left(1-a^{\alpha}\right)+\frac{a^{\alpha}}{5}\Big[\left(c_{m+1,n}^{\alpha(0)}+c_{m,n+1}^{\alpha(0)}+c_{m-1,n}^{\alpha(0)}+c_{m,n-1}^{\alpha(0)}\right)+\\&+\frac{1}{4}\left(c_{m+1,n+1}^{\alpha(0)}+c_{m+1,n-1}^{\alpha(0)}+c_{m-1,n+1}^{\alpha(0)}+c_{m-1,n-1}^{\alpha(0)}\right)\Big]-\sum_{\beta\neq\alpha}a^{\alpha\beta}c_{m,n}^{\beta}+\\&+\sum_{\beta\neq\alpha}\frac{a^{\alpha\beta}}{5}\Big[\left(c_{m+1,n}^{\beta(0)}+c_{m,n+1}^{\beta(0)}+c_{m-1,n}^{\beta(0)}+c_{m,n-1}^{\beta(0)}\right)+\\&+\frac{1}{4}\left(c_{m+1,n+1}^{\beta(0)}+c_{m+1,n-1}^{\beta(0)}+c_{m-1,n+1}^{\beta(0)}+c_{m-1,n-1}^{\beta(0)}\right)\Big]\end{aligned} \tag{9}$$

$$a^{\alpha\beta}=\frac{20D_{\alpha\beta}\Delta t}{h^2} \tag{10}$$

using the Moore automaton rule. The diffusion coefficients depend on the volumetric strain, [12].

The presented automata rules are a novel and alternative method to the simultaneous multicomponent flows that occur inside the material.

2.3. Evolution equations

Within a frame of continuous damage mechanics, the material deterioration can be entirely described by a scalar parameter composed of two parts – chemical and mechanical. The effective stress due to material degradation is, [4]:

$$\bar{\sigma} = \frac{\sigma}{\left(1-d_{ch}\right)\left(1-d_{m}\right)} \tag{11}$$

2.3.1. Chemical part

The diffusion processes through the porous material are very slow when compared to the rate of chemical reactions. The calculation recounted in [9] for similar chemical processes gave the Damköhler number of order 800, so much greater than one. This means that the chemical reaction process is strongly diffusion controlled. This is called an encounter complex where the formation of products is almost instantaneous. The actual rate of chemical reaction is limited by the slowest step – diffusion.

Considering a first order reaction kinetics, a formula similar to that which was proposed in [3] can be used:

$$\frac{dK}{dt} = \chi \left\langle c_a - c_{a0} \right\rangle_+ \tag{12}$$

where two parameters play an important role: they limit the concentration c_{a0} of the onset of the corrosion process and the coefficient χ is of a stoichiometric nature.

A simple linear dependence of the chemical damage parameter and the chemical reaction extent can be assumed:

$$d_{ch} = \xi K, \quad \xi \in \left(\xi_0, 1\right) \tag{13}$$

where ξ_0 stands for maximum material damage or residual strength of the material due to its non-homogeneity. A similar idea has been presented in [8].

2.3.2. Mechanical part

The mechanical damage parameter is defined by the formula in terms of an equivalent tensile strain, [6]:

$$d_m = 1 - \frac{\eta_0}{\eta}\left[1-\alpha_m\right] + \alpha_m \exp\left[\beta_m\left(\eta_0 - \eta\right)\right] \quad \eta(\varepsilon) = \sqrt{\frac{1}{E_0}\boldsymbol{\varepsilon} : \mathbf{C_0} : \boldsymbol{\varepsilon}} \tag{14}$$

The above formula is well suited for the modeling of concrete under compression as well as under tension and was compared with the Eurocode nonlinear elastic-plastic prescription, [14].

3. Numerical examples

A reinforced concrete cross-section exposed to 10% ammonium nitrate (V) solution and flexure stress is considered. Two cases of environmental action are considered: the first without protection; the second with one side protected, Fig. 1.

All required material and process data were adopted from the author's previous works, [12], or from numerical simulation of laboratory experiments on cementitious samples, [10]. The cement characteristics from [15] are recalculated here onto concrete characteristics.

3.1. Cross-section damage

The concentration contour lines were obtained as a solution of the transport equations with the use of the cellular automata. The reaction products are calcium nitrate and ammonia with a residual strength of the solid phase, this indicates the deterioration of the material.

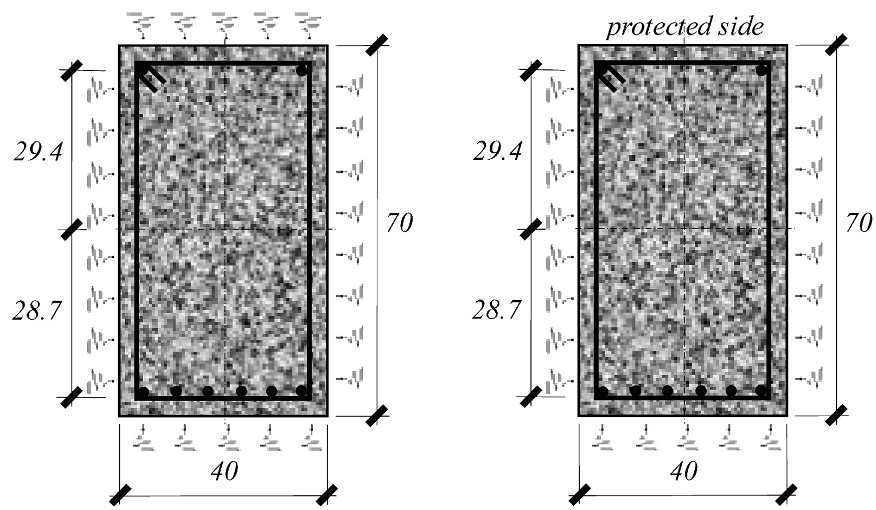

Fig. 1. A cross-section of RC beam: without protection (left); with one side protected (right)

The contour lines of the accumulative damage parameter are presented in Fig. 2. The solution for the case without protection demonstrates a lack of horizontal symmetry due to the mechanical load and different damage rate from the tensioned side in relation to the compressed side. The comparison of the solutions with different protections clearly shows the influence of boundary conditions on the actual form of cross-section damage. The bearing capacity of the RC cross-section comes from a combined action of the reinforcement and the compressed zone of concrete. Therefore, the damage processes in the compressed zone of the cross-section can considerably influence its bearing capacity.

3.2. Interaction surfaces

The cross-section bearing capacity decreases as a consequence of the material damage. The determination of cross-sectional forces in ultimate limit state is very important from the point of view of structural engineering. To assess limit values of the forces, the effective stress should be integrated over the cross-section area. The more general picture of limit values can be presented by interaction surfaces, or, due to poor visibility of 3D objects in 2D presentation, their sections commonly named the interaction curves.

However, the stress integration is not a standard procedure here for two reasons. Firstly, the effective stress state always depends on both space variables. In such cases, the ordinary integration procedures commonly employed in structural mechanics are useless. Secondly, due to stress softening, both in tension and compression, the ultimate values of cross-sectional forces are obtained for imminent but not exactly limit strains. The use of limit strains as prescribed by Eurocode for standard cases yields partially non-convex interaction curves. This is not an exact denouement to the problem, but such an erroneous solution can be found in several research papers ([7], for instance).

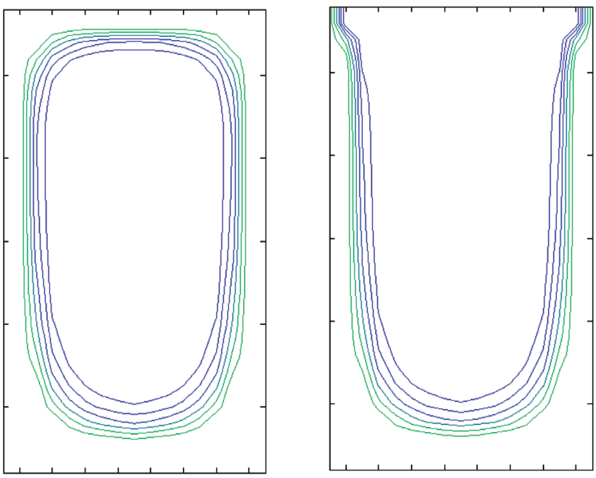

Fig. 2. Contour lines of damage parameter: without protection (left); with one side protected (right).

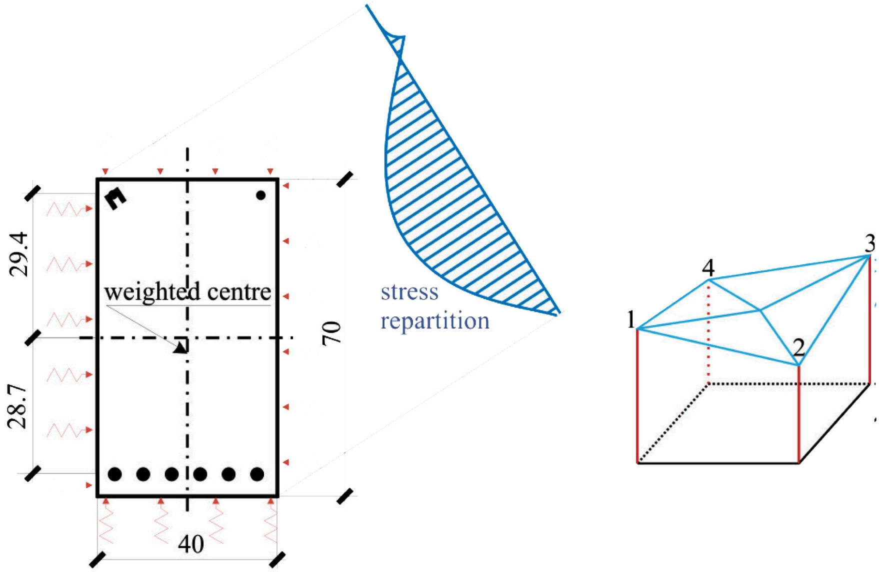

Fig. 3. A nominal stress repartition and stress integration method

A method of stress integration adopted here uses triangularisation based on the cellular automata discretization (Fig. 3). Using linear approximation, we get simple formulae for the finite difference resultant and its position:

$$\sigma_m = \sum_{i=1}^{4} \sigma_i, \quad S = \frac{1}{4}\Delta x^2 \sigma_m,$$
$$y_S = \frac{\Delta x}{24}\sum_{i=1}^{4}(-1)^i \frac{\sigma_i}{\sigma_m}, \quad z_S = \frac{\Delta x}{24}\sum_{i=1}^{4}(-1)^{(i+\mathrm{mod}(i,2)/2}\frac{\sigma_i}{\sigma_m} \tag{15}$$

The interaction curves are a solution of an inverse problem. For a given strain repartition, an appropriate stress repartition is calculated and integrated. In this way, a point in cross-sectional space is created. The interaction curves are simply a convex hull of all possible interaction points. To complete the task, a sufficiently dense, computer-generated set of possible strain repartition should be used.

The interaction curves of axial force and bending moment, (N–M_y), result from strain repartitions conserving symmetry, with the neutral axis perpendicular to the cross-section symmetry axis. The interaction curves of bending moments, (M_y–M_z), require an additional loop of iterations to fulfill the condition of zero axial force.

The interaction curves evolve over time. In Fig. 4, N–M_y and M_y–M_z curves are presented for the case without protection, and in Fig. 5, for the case with one side protected.

Due to ongoing material deterioration, the residual bearing capacity of the cross-section diminishes and the interaction curves shrink over time. Protection of one side of the cross-section results in smaller damage to the compression zone and a much greater bending moment capacity. The difference, however, is less visible on M_y–M_z curves.

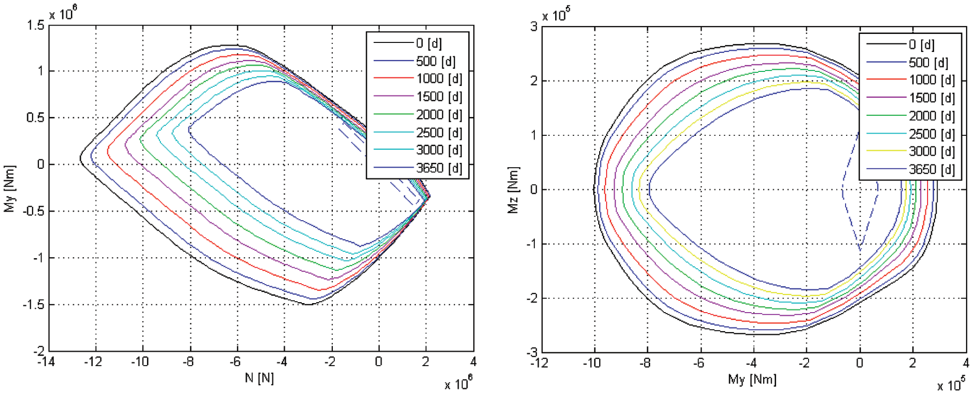

Fig. 4. Interaction curves N–M_y (left) and M_y–M_z (right), no protection

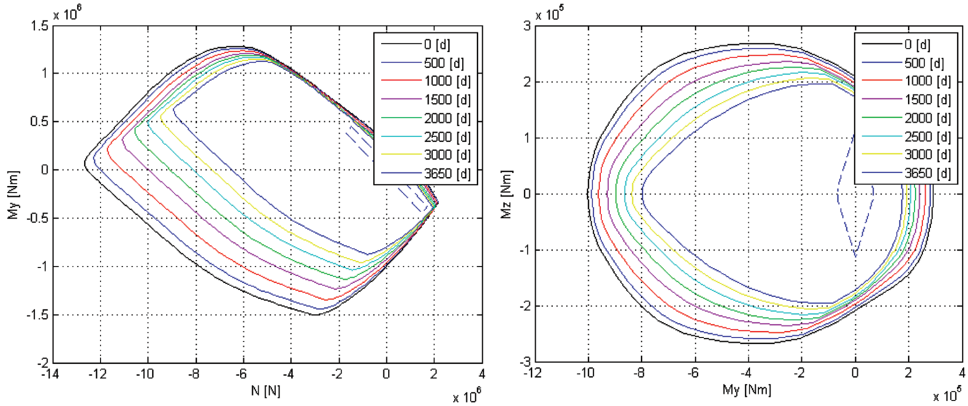

Fig. 5. Interaction curves N–M_y (left) and M_y–M_z (right), one side protected

4. Conclusions

Despite the many simplified assumptions adopted, the physical and chemical modelling of concrete corrosion presented here seems to be adequate to reproduce the characteristic material damage as well as the synergetic action of the environmental and mechanical load. The material and process parameters used in calculations were collected from various experimental works presented by other researchers so the results presented here have an informative character only.

Cellular automata are a robust tool for numerical analysis of the transport equations as well as stress integration. The existing ‘classical’ methods (Alternating Implicit Direction method, for instance) can be successfully replaced by this 60-year-old but novel method.

Most notably, to author’s knowledge this is the first study to simulate the long-term effects of concrete corrosion for different boundary conditions on the load-bearing capacity of the structural member cross-section.

References

[1] Bažant Z.P., Hauggaard A.B., Baweja S., Ulm F.-J., *Microprestress-solidification theory for concrete creep. I: Aging and drying effects*, Journal of Engineering Mechanics, Vol. 123(11), 1997, 1188-1194.

[2] Cervera M., Oliver J., Prato T., *Thermo-chemo-mechanical model for concrete. II: Damage and creep*, Journal of Engineering Mechanics, Vol. 125(9), 1999, 1028-1039.

[3] Comi C., Kirchmayr B., Pignatelli R., *Two-phase damage modeling of concrete affected by alkali–silica reaction under variable temperature and humidity conditions*, International Journal of Solids and Structures, Vol. 49, 2012, 3367-3380.

[4] Kattan P.I., Voyiadjis G.Z., *Decomposition of damage tensor in continuum damage mechanics*, Journal of Engineering Mechanics, Vol. 129(9), 2001, 940-944.

[5] Kubik J., *Przepływy wilgoci w materiałach budowlanych*, Oficyna Wyd. Politechniki Opolskiej, Opole 2000.

[6] Kuhl D., Bangert F., Meschke G., *Coupled chemo-mechanical deterioration of cementitious materials. Part I: Modeling*, International Journal of Solids and Structures, Vol. 41, 2004, 15-40.

[7] Papanikolaou V.K., *Analysis of arbitrary composite sections in biaxial bending and axial load*, Computers and Structures, Vol. 98-99, 2012, 33-54.

[8] Saetta A.V., Scotta R., Vitaliani R., *Mechanical behavior of concrete under physical-chemical attacks*, Journal of Engineering Mechanics, Vol. 124(10), 1998, 1100-1109.

[9] Samson E., Marchand J., *Modeling the transport of ions in unsaturated cement-based materials*, Computers and Structures, Vol. 85, 2007, 1740-1756.

[10] Schneider U., Chen S.-W., *Deterioration of high-performance concrete subjected to attack by the combination of ammonium nitrate solution and flexure stress*, Cement and Concrete Research, Vol. 35, 2005, 1705-1713.

[11] Xi J., Willam K.J., Frangopol D.M., *Multiscale modeling of interactive diffusion processes in concrete*, Journal of Engineering Mechanics, Vol. 126(3), 2000, 258-265.

[12] Zaborski A., *Zastosowanie automatów komórkowych do numerycznej symulacji korozji betonu pod obciążeniem*, Technical Transactions, series Mechanics, Vol. 107(9), 2010, 147-158.

[13] Zaborski A., *Corrosion of reinforced concrete due to stress-assisted diffusion*, Archive of Civil Engineering, Vol. 41(3), 1995, 447-460.

[14] Zaborski A., *Symulacja numeryczna wpływu korozji chemicznej betonu na nośność elementów żelbetowych*, Ochrona przed Korozją, Vol. 6, 2012, 279-281.

[15] Zaborski A., *Zmiany nośności przekroju żelbetowego wynikające z postępującej degradacji chemiczno-mechanicznej betonu*, Przegląd Budowlany, Vol. 5, 2014, 73-75.